Scattering from supramacromolecular structures

Carlos I. Mendoza and Carlos M. Marques
LDFC-UMR 7506, 3 rue de l'Université, 67084 Strasbourg Cedex, France
(Received 23 April 2002; published 21 November 2002)

We study theoretically the scattering imprint of a number of branched supramacromolecular architectures, namely, polydisperse stars and dendrimeric, hyperbranched structures. We show that polydispersity and nature of branching highly influence the intermediate wave vector region of the scattering structure factor, thus providing insight into the morphology of different aggregates formed in polymer solutions.

DOI: 10.1103/PhysRevE.66.051805 PACS number(s): 36.20.Ey, 61.25.Hq

I. INTRODUCTION

Scattering by light, x rays or neutron radiation provides a fundamental tool to investigate the shapes and statistical nature of large molecules in solution [1]. For objects of fixed shape, like spherical, ellipsoidal, or cylindrical colloids, the scattering functions are known and can easily be compared to experimental data, thus allowing for a determination of shapes and relevant dimensions of the objects in a given experimental sample. For objects of a relatively simple geometry, but with a fluctuating nature, such as polymer chains or semiflexible rods the scattering spectra contains not only information about the average shape of the mass distribution but carries also a signature of the conformational disorder determined by the nature of the thermodynamic fluctuations. For flexible polymers, for instance, one can determine from the scattering data whether monomer-monomer excluded volume interactions are relevant or not in a particular, given solvent.

Association of fixed-shape objects, such as the aggregation of spherical colloids that lead to fractal DLA (diffusion-limited aggregation) structures [2], brings also some degree of disorder into the spatial distribution of the scattering elements. Although the object as a whole does not fluctuate in time, the spatial distribution of the scattering elements is statistically fixed by the aggregation process itself. DLA and other related processes have been shown to lead to self-similar aggregates [3], where the frozen position correlations $g(r)$ between different elements at a distance r are described by a power law $g(r)\sim r^{-m}$. It is well known that the scattering data from these objects also carries the signature of the exponent m, thus providing some insight on the type of the aggregation process ruling the solution behavior.

When the aggregation process involves fluctuating objects, the scattering function carries information both on the connectivity between different scattering elements and on the statistics of the fluctuations. In this paper we discuss the interplay between these two factors by studying a number of branched polymer structures. Branched polymers are arguably the larger class of systems of connected fluctuating elements, systems that also include aggregates of soft gel beads, emulsion droplets, and others. In many polymer or polymerlike structures, control of the branching chemistry allows for a careful choice of the connectivity, like in dendrimers [4,5] or in star-branched polymers [6,7], and to some extent in dendrimeric (also called hyperbranched) polymers [8–10]. Geometries with higher degree of disorder are obtained by spontaneous aggregation in solutions of polymers carrying sticking groups, and by random branching during polymerization growth. This leads to a great diversity in the connections and to a polydispersity in sizes of the constitutive elements. In order to clarify the role of each of these factors in shaping the scattering functions, we explore a number of structures obtained by variations of starlike polymers: stars with polydisperse arms, and dendrimeric polymers with different degrees of polydispersity.

The paper is organized as follows. In Sec. II we recall some basic general features of the scattering amplitude for well known, fixed-shape and fluctuating objects. Section III discusses the scattering function of Gaussian branched and hyperbranched structures, and also discusses qualitatively the effects of excluded volume. Finally, in the conclusions we discuss the different scattering signatures according to branching structure and statistical nature of the fluctuations.

II. SCATTERING FROM SIMPLE POLYMER ARCHITECTURES

The structure factor of an aggregate is given by

$$S(\mathbf{q})=\frac{1}{\mathcal{N}}\left\langle \sum_{n,m=1}^{\mathcal{N}} \exp\{i\mathbf{q}\cdot(\mathbf{R}_n-\mathbf{R}_m)\}\right\rangle, \tag{1}$$

where $\mathcal{N}$ is the number of scattering units in the aggregate (monomers), $\mathbf{R}_i$ is the position of the ith scattering unit, the ensemble average is denoted by $\langle\cdots\rangle$, and $\mathbf{q}$ is the momentum transfer given by $\mathbf{q}=\mathbf{q}_s-\mathbf{q}_i$. Here $\mathbf{q}_i$ and $\mathbf{q}_s$ are the wave vectors of the incident and scattered fields. For elastic scattering $|\mathbf{q}_s|=|\mathbf{q}_i|=2\pi/\lambda$, where λ is the wavelength of the incident wave. Hence, $q\equiv|\mathbf{q}|=(4\pi/\lambda)\sin\theta/2$, with θ the scattering angle.

An illustration of the form of the scattering amplitude for two objects of well defined shapes is shown in Fig. 1. In this figure, the spherically averaged scattering function of an infinitely thin uniform rod of length L is compared to that of an uniform sphere of radius $R=L/2$. For simplicity both curves have been normalized to 1 at the origin. The curve corresponding to the rod shows a power law region with slope -1 for large wave vector q, reflecting the unidimensional nature of the rod. Indeed, for a mass density distribution of the form $g(r)\sim r^{-(3-D)}$, where D is the fractal dimension of the object, one expects the scattering behavior $S(\mathbf{q})\sim q^{-D}$. For rods, $D=1$, and $S(\mathbf{q})\sim q^{-1}$. This holds for spatial scales $r\ll R_g$ or reciprocal lengths $qR_g\gg 1$, where R_g is the radius

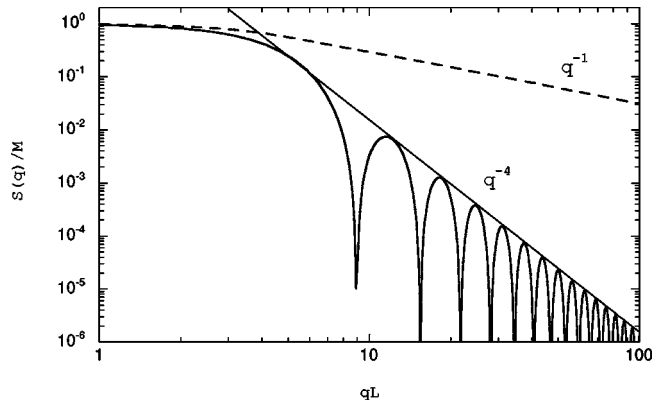

FIG. 1. Sketch of the scattering intensity for a uniform rod of length L and mass M (dashed line) and a uniform sphere of radius $R=L/2$ and the same mass (solid line). A straight line with slope -4 is also shown.

of gyration of the object $R_g^2=(1/2\mathcal{N}^2)\Sigma_{i,j}(R_i-R_j)^2$. For rods, $R_g^2=L^2/12$. At small wave vectors $qR_g\ll 1$, $S(\mathbf{q})$ rolls off into a plateau (Guinier) region. Deviations from the plateau value give a measure of the radius of gyration of the object. In this region $S(\mathbf{q})\sim 1-q^2R_g^2/3$. The structure factor of the sphere also shows a Guinier zone that rolls off from the plateau at a smaller wave vector q indicating that the radius of gyration of this sphere is larger than the radius of gyration of the rod. For larger values of q, the sphere structure factor oscillates, the separation between the peak positions being also a measure of the size of the sphere. The decaying envelope has a slope -4, typical of objects with sharp interfaces.

As an example of the scattering function of fluctuating objects, we consider the structure factor of a linear Gaussian polymer with $P\times N$ monomers and of an uniform star of P arms of N monomers each one [see Fig. 2 and also Eq. (A10)]. For the linear polymer, the large q behavior follows a power law with a slope -2, a manifestation of the fractal dimension of a Gaussian chain, $D=2$. The same behavior is seen at large wave vectors for the star scattering function.

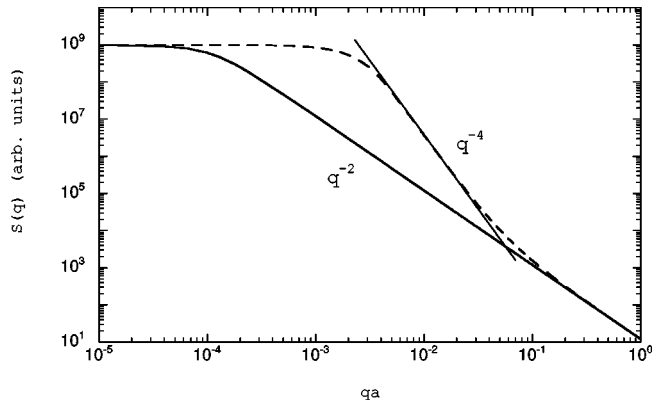

FIG. 2. Scattering intensity for a linear Gaussian polymer of PN monomers (solid line) and a Gaussian star of $P=10^3$ arms each one of $N=10^6$ monomers (dashed line). A straight line with slope -4 is also shown.

However, the star shows a second power law region with slope -4 before saturating at the plateau value. Notice that a steepest curve is necessary to connect a plateau extending further in q (the radius of gyration of the star is smaller than the radius of gyration of the linear polymer) to a coincidental high q region in which both, the polymer and the star, have the same local statistical structure. Quantitatively, the value -4 is related to the average concentration profile. Indeed, it can be shown [11] that, when scattering from an inhomogeneous region of average concentration $\phi(r)$ dominates the spectrum, $S(\mathbf{q})$ is calculated from

$$S(\mathbf{q})\sim\frac{1}{\mathcal{N}}\left[\int_0^\infty r^2dr\,\frac{\sin qr}{qr}\,\phi(r)\right]^2. \tag{2}$$

For a Gaussian star polymer, the average concentration profile is given by $\phi(r)=3P/(2\pi a^2 r)\mathrm{erfc}(r/2R_g)$, where r is the distance from the center of the star, a is the monomer size, and $\mathrm{erfc}(x)$ is the complementary error function [12]. Equation (2) thus leads to

$$S(\mathbf{q})\sim\frac{P}{Nq^4},\quad 1\ll qR_g\ll P^{1/2}. \tag{3}$$

Note that this form crosses over correctly from the plateau region $S(q)\sim P\times N$ at $q\sim R_g^{-1}$ to the high q-region $S(q)\sim q^{-2}$ at $q\sim P^{1/2}R_g^{-1}$.

Even in the absence of an exact form for the radial concentration profile, a general argument can be made [13] in order to extract the value of the intermediate slope. For a star with P arms, the average concentration inside an infinitesimal spherical shell of volume $4\pi r^2dr$ and radius r, centered on the star, is given by

$$\phi(r)=PdN(r)/(4\pi r^2dr), \tag{4}$$

with $dN(r)$ is the average number of monomers per arm in the shell. For a Gaussian arm $N(r)\simeq 3r^2/a^2$ and one easily recovers the exact result for the concentration in the scaling regime $r\ll R_g$. The Daoud and Cotton argument (4), combined with Eq. (2) also allows to compute the intermediate regime of the scattering factor of a star in a good solvent, where excluded volume interactions are important. In this case, the star can be described as a semidilute solution, with a local, position dependent screening length $\xi(r)$. Pictorially, this is represented by arms made of a succession of blobs of increasing size $\xi(r)$. The arms are stretched and within a distance r from the center one finds $N(r)\simeq(r/a)^{5/3}P^{-1/3}$ monomers, the size of the star in a good solvent being $R_{\mathrm{star}}\simeq N^{3/5}P^{1/5}$. It follows that the average concentration varies radially as $\phi(r)\sim P^{2/3}r^{-4/3}$ and the intermediate regime is described by

$$S(\mathbf{q})\sim\frac{P^{1/3}}{Nq^{10/3}},\quad 1\ll qR_{\mathrm{star}}\ll P^{2/5}. \tag{5}$$

For higher wave vectors, $qR_{\mathrm{star}}\gg P^{2/5}$, the function $S(\mathbf{q})$ crosses over to a slope $-5/3$ indicative of the local excluded volume statistics of the arms [14].

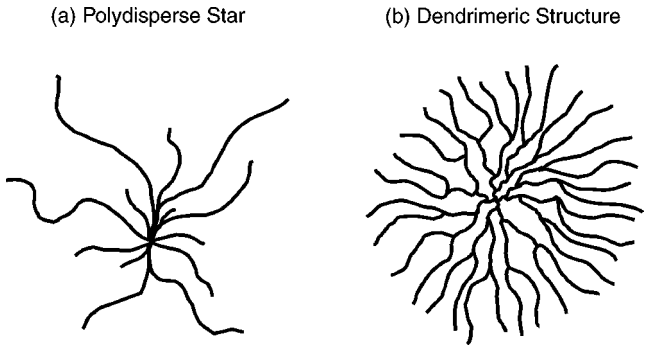

FIG. 3. Schematic representation of (a) Polydisperse stars and (b) Dendrimeric structures formed by connecting linear polymers.

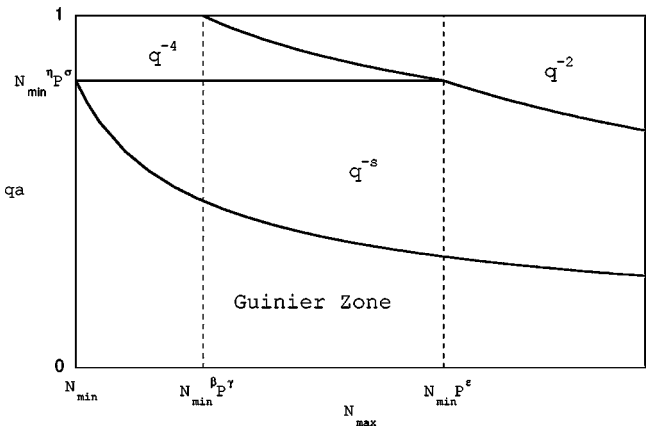

FIG. 4. Diagram showing the different scaling regimes of the scattering function for: polydisperse stars in θ solvent [$\beta=-1/(m-1)$, $\gamma=m/(m-1)$, $\epsilon=\gamma$, $\eta=-1/2$, $\sigma=0$, and $s=2(2-1/m)$], polydisperse stars in athermal solvent [$\beta=-4/(6m-5)$, $\gamma=1/3(6m-1)/(6m-5)$, $\epsilon=2\gamma$, $\eta=-3/5$, $\sigma=-1/5$, *and* $s=10/3(1-2/(6m-1))$], *dendrimeric structures in* θ *solvent* [$\beta=1/(2m+1)$, $\gamma=2m/(2m+1)$, $\epsilon=\gamma$, $\eta=-1/2$, $\sigma=0$, *and* $s=2(2+1/m)$], *and dendrimeric structures in athermal solvent* [$\beta=1/(2m+1)$, $\gamma=(1/3)2m/(2m+1)$, $\epsilon=2\gamma$, $\eta=-3/5$, $\sigma=-1/5$, *and* $s=10/3(1+2/(6m+1))$].

III. BRANCHED STRUCTURES

The objective of this section is to show how the internal branched structure of the aggregate modifies the form of the structure factor. In order to do this, we consider two different types of aggregates, (a) polydisperse stars, and (b) dendrimeric structures (see Fig. 3).

The method of calculation for the structure factor of aggregates (a) and (b) starts by considering an arbitrary aggregate whose scattering function is known. If a new arm is added to the structure, the scattering function that accounts for the new arm can be calculated in terms of the known scattering function plus corrections due to the correlations between the monomers of the new arm with themselves and with all the monomers of the previous aggregate. A more detailed discussion of the procedure is given in Appendix A where the structure factor of a dendrimer of two generations is computed in terms of the structure factor of a monodisperse star.

A. Polydisperse stars

Consider a star-branched polymer made of P_1 arms of N_1 monomers, P_2 arms of N_2 monomers and so on [see Fig. 3(a)]. The structure factor of this aggregate is

$$S(\mathbf{q})=\frac{1}{\sum_{i=1}^{G} P_i N_i}\sum_{p,q=1}^{G} P_p P_q \frac{N_p N_q}{x_p x_q}(\exp(-x_p)-1)$$

$$\times(\exp(-x_q)-1)+\frac{1}{\sum_{i=1}^{G} P_i N_i}\sum_{q=1}^{G} P_q \frac{N_q^2}{x_q^2}$$

$$\times[2(\exp(-x_q)-1+x_q)-(\exp(-x_q)-1)^2]. \tag{6}$$

Here, G is the number of different lengths, $x_q=q^2a^2N_q/6$. Note that this expression can be decomposed, as for the monodisperse star, in a contribution from the average concentration of the star plus contributions from the fluctuations. However, as we will see below, the general shape of the scattering curve now exhibits a richer behavior. The low wave vector and the high wave vector regions still present the usual Guinier roll off from a plateau and a ''-2 slope,'' respectively. The signature of the star polydispersity is carried by the shape of the intermediate scattering region. Consider the case of arm-size polydispersity. Here, we take the star to be made of G different stars, each of them with equal arm number P but an arm-size distribution N_i. For the form $N_i=N_{max}i^{-2m}$, where $m\geqslant 0$, i runs from 1 to G and N_{max} is the number of monomers of the largest arms, the radius of gyration of each arm is $R_i=\text{const}\times i^{-m}a$, and the average concentration can be written as [15]

$$\phi(r)=\sum_i \phi_i(r)=\frac{3P}{2\pi a^2 r}\sum_i \text{erfc}(r/2R_i)$$

$$\simeq \frac{3P}{2\pi a^3}\frac{(2\times\text{const})^{1/m}\Gamma\left(\frac{1+m}{2m}\right)}{\sqrt{\pi}}\left(\frac{a}{r}\right)^{(m+1)/m}, \tag{7}$$

where Γ is the gamma function $\Gamma(a)=\int_0^\infty dx x^{a-1}\exp\{-x\}$. If the exponent m is very large, only the P largest arms contribute to the concentration profile which is very similar to a monodisperse star. As the distribution width increases, the smaller arms start to significantly contribute to the profile. In this case, several different regimes can be identified, as shown in Fig. 4. By inserting the continuous limit of Eq. (7) in Eq. (2) we find an intermediate regime that scales as $S(q)\sim q^{-2(2-1/m)}$, for $m\geqslant 1/2$. This means that for the polydispersity considered here, the exponent varies from 0 when $m=1/2$ to -4 when $m\to\infty$. Interestingly, a second intermediate regime develops due to the finite distribution of the arm polydispersity. When the size of arms has a finite small cutoff at $N_{min}=N_G$, the polydisperse star consist of two parts:

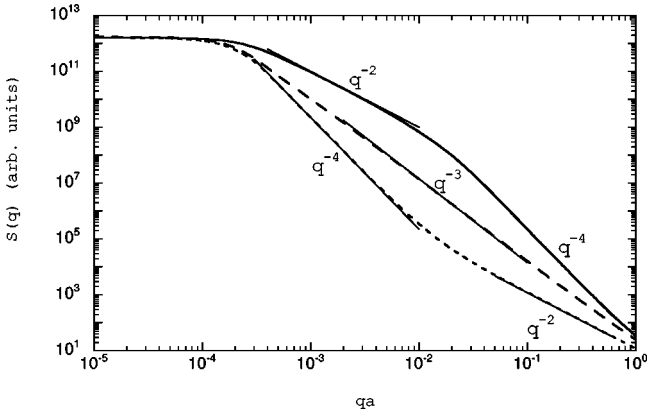

FIG. 5. A comparison of the scattering intensity as a function of the scattering vector in a log-log scale for polydisperse stars of the same mass in θ solvent. The parameters for the polydispersed stars are $G=100$, $P_i=10^4$, and $N_i \sim 10^8 i^{-2m}$ with $m=1$ (solid line), $m=2$ (dashed line), and $m \to \infty$ (dotted line). This last case corresponds to a uniform star of $P_G=10^4$ arms. Straight lines with slopes -4, -3, and -2 are also shown.

the outer polydisperse shell and a central starlike core. This second intermediate regime therefore appears at length scales smaller than the length of the smaller arms and follows the usual q^{-4} scaling. At low wave vectors q the spectrum shows a Guinier plateau. The transition point between the Guinier zone and the first intermediate region occurs at $(qR_g)^2 \sim 1$ as can be verified by inserting the exact form of Eq. (7) in Eq. (2) and exploring the small q limit of the resulting expression. The radius of gyration of the polydisperse star is $R_g^2=[\int_0^\infty dr\, r^4 \phi(r)]/[\int_0^\infty dr\, r^2 \phi(r)] = 3R_1^2[\Sigma_i i^{-4m}]/[\Sigma_i i^{-2m}]$, where $R_1 \sim a N_1^{1/2}$ is the gyration radius of the largest arm. For large values of m one recovers the limit of the monodisperse star $R_g^2=3R_1^2$. Written in terms of the monomer size a, the transition point between the Guinier zone and the first intermediate regime occurs at $(qa)^2 \sim 1/N_{max}$, where $N_{max}=N_1$ is the number of monomers of the largest arms. The transition point between the two intermediate regions occurs at $(qa)^2 \sim 1/N_{min}$, where $N_{min}=N_G$ is the number of monomers of the shortest arms. Finally, the transition between the second intermediate region and the region where fluctuations dominate occurs at $(qa)^2 \sim P/N_{max}(N_{max}/N_{min})^{1/m}$. One can see that the region where fluctuations dominates appears only if $N_{max} > P^{m/(m-1)} N_{min}^{-1/(m-1)}$. If the exponent m is larger than one and the number of monomers N_{max} is very large, $N_{max} \gg N_{min} P^{m/(m-1)}$, the region with slope q^{-4} disappears and one crosses over directly to the region dominated by fluctuations with slope q^{-2}. The transition point then occurs at $(qa)^2 \sim P^{m/(m-1)}/N_{max}$ (see Fig. 4). For values of m between 1 and 1/2, the scattering function always crosses from the regime $S(q) \sim q^{-2(2-1/m)}$ to a regime $S(q) \sim q^{-4}$ independently of the number of monomers N_{max}. Examples of some of these cases are presented in Fig. 5 (see note Ref. [15]). In the limit $m=1/2$ the scattering function does not exhibit a developed scaling but rolls over gently from the Guinier plateau to the large wave vector limit of slope -2.

For a polydisperse star in a good solvent a Daoud-Cotton argument can also be applied to determine the scattering regimes. Let $p(r)$ be the number of arms at distance r from the center. Then, the local correlation length is set by $\xi(r) = r p(r)^{-1/2}$ and the concentration is $\phi(r)=p(r)^{2/3} r^{-4/3}$. In the infinitesimal shell of volume $dV=4\pi r^2 dr$, there are then $dn=p(r)^{-1/3} r^{2/3} dr$ monomers in one arm. By knowing the polydispersity of the chains $p(n)$ one can compute the function $p(r)$ and extract the concentration. If we choose, as for the precedent Gaussian example, $N_i=N_{max} i^{-2m}$, and a constant arm number of each length, $P_i=P$, we get in the continuous limit $p(n)=P(n/N_{max})^{-1/2m}$, leading to $p(r) \sim r^{-5/(6m-1)}$. Correspondingly, the concentration scales as $\phi(r) \sim r^{-\alpha}$ with the exponent $\alpha=\frac{2}{3}[2+5/(6m-1)]$ and the scattering from that intermediate region scales as $S(q) \sim q^{-s}$, with exponent $s=\frac{10}{3}[1-2/(6m-1)]$. In the limit where m is very large one recovers the usual intermediate slope $s=10/3$. As m decreases we reduce the intermediate slope, as for the Gaussian case. The transition point between the Guinier zone and this region occurs at $(qa)^{5/3} \sim 1/(N_{max} P^{1/3})$. As in the Gaussian case, we find a second intermediate region that scales as $S(q) \sim q^{-10/3}$. The transition point between the two intermediate regions occurs at $(qa)^{5/3} \sim 1/(N_{min} P^{1/3})$. Finally, the transition between the second intermediate region and the fluctuating regime occurs at $(qa)^{5/3} \sim P^{1/3}/N_{max}(N_{max}/N_{min})^{4/(6m-1)}$. These results are shown in Fig. 4. One can see that the region where fluctuations dominates appears only if $N_{max} > P^{1/3(6m-1)/(6m-5)} N_{min}^{-4/(6m-5)}$. If the exponent $m \geqslant 5/6$ and the number of monomers N_{max} is very large, $N_{max} \gg N_{min} P^{2/3(6m-1)/(6m-5)}$, the region with slope $q^{-10/3}$ disappears and one crosses over directly to the region dominated by fluctuations with slope $q^{-5/3}$. The transition point then occurs at $(qa)^{5/3} \sim P^{(2m+1)/(6m-5)}/N_{max}$. Again, by choosing the value of m between ∞ and 5/6, it is possible to obtain scattering functions with intermediate slopes ranging from the monodisperse star value of $-10/3$ to $-5/3$ slope. For values of m between 5/6 and 1/2, the scattering function always crosses from the regime $S(q) \sim q^{-10/3(1-2/(6m-1))}$ to a regime $S(q) \sim q^{-10/3}$ independently of the number of monomers N_{max}.

B. Dendrimeric Structures

These structures are formed by starting from a uniform star of $P_1=P$ arms of N_1 monomers each one, and branching each arm twice so that in the second generation there are $P_2=2P_1$ arms of length N_2. We then branch each of the newest arms twice so that in the third generation there are $P_3=2P_2=2^2P_1$ arms of length N_3. We repeat this process up to any desired number of generations [see Fig. 3(b)]. This means that the number of arms in each generation is $P_i = 2^{i-1}P$. As in the case of the polydisperse stars, for a large number of arms and generations, asymptotic shapes can be reached for particular types of polydispersity distributions. Let us consider the case of a dendrimer of G generations with arm-size polydispersity of the form $\mathcal{N}_i = 2^{2m(i-1)} \mathcal{N}_{min}$, where $\mathcal{N}_i = \Sigma_{j=1}^{i} N_j$ is the sum of monomers per arm from generation 1 up to generation i. By choosing $m \geqslant 1/2$, we assure that the first generation always

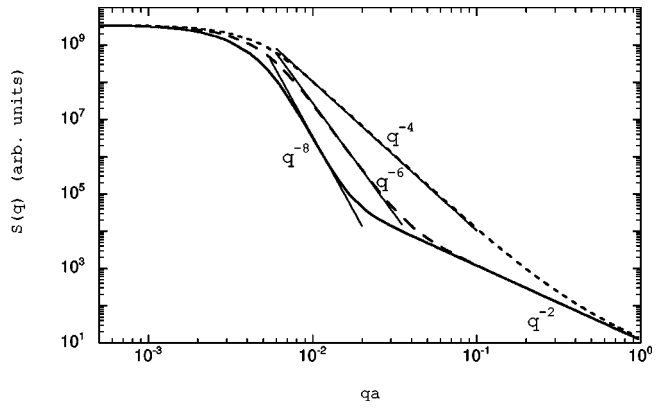

FIG. 6. A comparison of the scattering intensity as a function of the scattering vector in a log-log scale for dendrimers with the same mass. The parameters used were $G=10$, $P=20$, and $\mathcal{N}_i \sim 10^3 i^{-2m}$ with $m=1/2$ (solid line), $m=1$ (dashed line), and $m \to \infty$ (dotted line). This last case corresponds to a uniform star of $P_G=20\times 2^9$ arms. Straight lines with slopes -8, -6, and -4 are also shown.

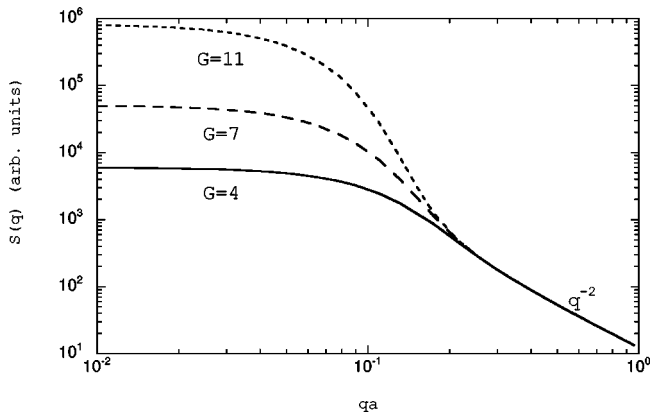

FIG. 7. A comparison of the scattering intensity as a function of the scattering vector in a log-log scale for a dendrimeric structure of different number of generations, G. The parameters for the dendrimer are $N_i=100$, $P=20$.

has the smallest number of monomers per arm. By using arguments similar to those for the polydisperse star, we find for the Gaussian dendrimer, an average concentration $\phi(r) \sim r^{-(1-1/m)}$, that gives rise to an intermediate scaling regime $S(q) \sim q^{-2(2+1/m)}$ [16]. Again, if m is very large, only the last generation contributes to the scattering, which is similar to the monodisperse star with P_G arms. As m decreases, the first generations start to contribute significantly, modifying the slope of the scattering curves that reaches the steepest value of -8 when $m=1/2$. The transition point between the Guinier zone and this region occurs at $(qa)^2 \sim 1/\mathcal{N}_{max}$, where $\mathcal{N}_{max}=\mathcal{N}_G$. Also, there is a second intermediate region which scales as $S(q) \sim q^{-4}$. The transition point between these two intermediate regions occurs at $(qa)^2 \sim 1/\mathcal{N}_{min}$, where $\mathcal{N}_{min}=\mathcal{N}_1$ (see Fig. 4). Finally, the transition between the second intermediate region and the fluctuating regime occurs at $(qa)^2 \sim P/\mathcal{N}_{max}(\mathcal{N}_{max}/\mathcal{N}_{min})^{-1/2m}$. The region where fluctuations dominates appears only if $\mathcal{N}_{max} > P^{2m/(2m+1)}\mathcal{N}_{min}^{1/(2m+1)}$. The regime with $S(q) \sim q^{-4}$ disappears when $\mathcal{N}_{max} \sim \mathcal{N}_{min}P^{2m/(2m+1)}$. In this case the transition point between the region with $S(q) \sim q^{-2(2+1/m)}$ and the fluctuating regime occurs at $(qa)^2 \sim P^{m/(m+1)}/\mathcal{N}_{max}(\mathcal{N}_{max}/\mathcal{N}_{min})^{1/2(m+1)}$. Note that for large $\mathcal{N}_{max}$ and by tuning m between ∞ and 1/2, it is possible to obtain scattering functions with intermediate slopes ranging from the monodisperse star value of -4 to -8 slope. In Fig. 6 we show examples of some of these cases.

Applying a Daoud-Cotton argument to the case of dendrimers in good solvent we determine the corresponding scaling regimes. In this case, $p(r) \sim r^{5/(6m+1)}$. Correspondingly, the concentration scales as $\phi(r) \sim r^{-\alpha}$, with $\alpha=\frac{2}{3}[2-5/(6m+1)]$ and the scattering from that intermediate region scales as $S(q) \sim q^{-s}$, with $s=\frac{10}{3}[1+2/(6m+1)]$. In the limit where m is very large one recovers the usual intermediate slope $s=10/3$. As m decreases we reduce the intermediate slope, as for the Gaussian case. The transition point between the Guinier zone and this region occurs at $(qa)^{5/3} \sim 1/(P^{1/3}\mathcal{N}_{max})(\mathcal{N}_{max}/\mathcal{N}_{min})^{-1/6m}$. As in the Gaussian case, we find another intermediate region that scales as $S(q) \sim q^{-10/3}$. The transition point between the two intermediate regions occurs at $(qa)^{5/3} \sim 1/(P^{1/3}\mathcal{N}_{min})$. Finally, the transition between the second intermediate region and the fluctuating regime occurs at $(qa)^{5/3} \sim P^{1/3}/\mathcal{N}_{max}(\mathcal{N}_{max}/\mathcal{N}_{min})^{-1/2m}$. These results are shown in Fig. 4. The region where fluctuations dominates appears only if $\mathcal{N}_{max} > \mathcal{N}_{min}^{1/(2m+1)}P^{2m/[3(2m+1)]}$. If $\mathcal{N}_{max}$ is very large, $\mathcal{N}_{max} \gg \mathcal{N}_{min}P^{4m/[3(2m+1)]}$, the region with slope $q^{-10/3}$ disappears and one crosses over directly to the region dominated by fluctuations with slope $q^{-5/3}$. The transition point then occurs at $(qa)^{5/3} \sim P^{(2m-1)/(6m+5)}/\mathcal{N}_{max}(\mathcal{N}_{max}/\mathcal{N}_{min})^{(2m-1)/[2m(6m+5)]}$. Again, by choosing the value of m between ∞ and 1/2, it is possible to obtain scattering functions with intermediate slopes ranging from the monodisperse star value of $-10/3$ to -5 slope.

The results for the scaling regimes and the transitions between these regimes for both, polydisperse stars and hyperbranched structures are summarized in Appendix B.

In Fig. 7 we plot the structure factor for Gaussian dendrimers with arms of equal size for all the generations. In this case a non-scaling regime is present between the Guinier zone and the high q region. This region shows a hump that reflects the fact that as we increase the number of generations, the outer core of the aggregate becomes very dense thus dominating the structure of the spectrum which resembles the one for a spherical shell. We see in Fig. 7 that the size of the hump increases as we increase the number of generations in qualitative agreement with the experimental results of Ref. [17]. Note that while growth of dendrimers to a high number of generations is usually hindered by steric reasons, a polydisperse dendrimer can grow indefinitely if the polydispersity is correctly tuned.

From the scattering curves of branched structures in which there is a q region where fluctuations dominate, we note that there is always an intermediate q region with a steeper slope than the corresponding one for a linear polymer. This can be understood by using a simple graphical

argument. Consider a linear Gaussian polymer of mass N. Its structure factor consist of a power law region with slope -2 and a Guinier zone for low wave vector q. Now, let us consider any branched Gaussian polymer. Its structure factor coincides, in slope and absolute value, with the one for the linear Gaussian polymer at short-wave lengths. This reflects the fact that the internal structure of the polymer is the same in both cases. If the branched polymer has the same mass than the linear one, both spectra must coincide in the plateau Guinier zone. However, since the radius of gyration of any branched polymer is always smaller than the corresponding one for the linear polymer, the Guinier zone must extend to a larger wave vector value, as shown for example in Fig. 2. Therefore, the only possible way of crossing from one region to the other is by an intermediate region with an average slope larger than the slope at short-wave lengths. This argument is also valid in good solvent conditions where the Gaussian model is not valid and monomer-monomer interactions play an important role.

IV. CONCLUSIONS

In this paper we have shown how different branched polymers give rise to different structure factors. This information can be used to probe the morphology of supramacromolecular aggregates. We have shown how the slope in the intermediate q region can be tailored according to the polydispersity in the length of the constitutive linear chains of the branched aggregates. In particular, for polydisperse stars we found scaling regimes with slopes ranging from -2 to -4 in θ solvent conditions and between $-5/3$ and $-10/3$ for athermal solvent. In the case of dendrimeric structures, scaling regimes ranging from -4 to -8 in θ solvent and between $-10/3$ and -5 for athermal conditions, although richer behavior was obtained for specific choices of the polydispersity parameters. We have shown using simple arguments that whenever there is a region where fluctuations dominate the scattering response, then the structure factor of branched structures always present an intermediate q regime with at least a small region where the slope in a log-log plot is larger than the corresponding slope of the linear polymer. This means that these aggregates are not strictly self-similar over the entire range of length scales $a<l<R_g$. Results presented in this paper can be qualitatively used as a guiding tool for exploring the branching morphology of aggregates according to the type of regimes presented in the scattering intensity curves. They also provide qualitative information from the analysis of the values of the slopes of the intermediate q regimes.

APPENDIX A: METHOD OF CALCULATION

In this appendix we outline the procedure to obtain the structure factor for the branched structures described in this paper by considering a specific example. Suppose a branched polymer that grows following a given rule like the one shown in Fig. 3(b). In this figure, we show a polymer that grows from a star of P_1 arms each one made of N_1 monomers. Each arm is then branched in two other arms made of N_2 monomers. Then, each arm of the newest generation is branched again in two arms and so on. The structure factor of the structure made of G generations is related to the structure factor of the structure made of $G-1$ generations by the equation

$$S_G(\mathbf{q}) = \frac{\sum_{i=1}^{G-1} P_i N_i}{\sum_{i=1}^{G} P_i N_i} S_{G-1}(\mathbf{q}) + S_{corr}(\mathbf{q}), \qquad \text{(A1)}$$

where P_i and N_i are the number of arms and monomers in the ith generation, respectively, $S_i(\mathbf{q})$ is the structure factor of the structure made of i generations and the *corrections*, $S_{corr}(\mathbf{q})$, are due to the correlations between the arms grown in the Gth generation with themselves and the rest of the arms. Assuming that $S_{G-1}(\mathbf{q})$ is known, the problem consist in calculate these corrections. Then, applying the procedure recursively, the structure factor of any structure made of an arbitrary number of generations can be calculated.

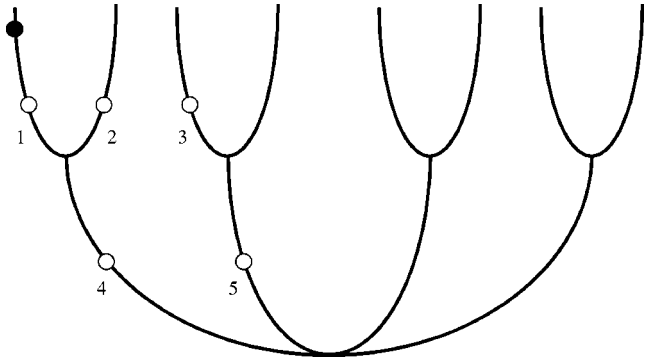

FIG. 8. Representation of a dendrimer with $P=4$ arms, and $G=2$ generations. The solid circle represents the location of monomer m and the open circles represent the locations of monomers n representatives of the different families.

Now we proceed with the calculation of the *corrections*. In order to show the general idea, we are going to treat the simple case of a dendrimer with $G=2$ generations (see Fig. 8). Any monomer m that belongs to the last generation ($G=2$) interacts with all other monomers of the structure. These interactions can be classified according to the relative location, in the structure, of the second monomer n with respect to to monomer m. This is shown in Fig. 8 where we classify the position of the second monomer in 5 different families. The monomers n of family 1 belongs to the same generation and to the same arm of monomer m. Family 2 comprises all the monomers n of the same generation of m but that belong to a different arm whenever this arm has a common origin with the arm where m is located. Family 3 consists of monomers n of the same generation of m and whose respective arms originate in different arms of the previous generation. For family 4 one monomer, say m, belongs to generation G and the other (n) belongs to generation $G-1$, and the arm where m is located originates in the arm where n is located. Finally, family 5 consists of monomers n of different generation than that of monomer m, and the monomer m cannot be

reached by going through the arm where n is located. All the monomers that participate in the corrections belong to one of these families. Contributions to the structure factor from a given family f are calculated from the expression

$$S^f_{corr}(\mathbf{q}) = \frac{1}{N_T}\sum_{m,n}\int d\mathbf{R}_m d\mathbf{R}_n G^f_{m,n}(\mathbf{R}_n,\mathbf{R}_m) \times \exp\{i\mathbf{q}\cdot(\mathbf{R}_n-\mathbf{R}_m)\}, \tag{A2}$$

where N_T is the total number of monomers, the sum runs over monomer m and n with at least one of them belonging to the latest generation ($G=2$), and $G^f_{m,n}(\mathbf{R}_n,\mathbf{R}_m)$ is the Green function of the f family given by

$$G^1_{m,n}(\mathbf{R}_n,\mathbf{R}_m) = G(\mathbf{R}_n,\mathbf{R}_m;m-n), \tag{A3}$$

$$G^2_{m,n}(\mathbf{R}_n,\mathbf{R}_m) = G(\mathbf{R}_n,\mathbf{R}_m;m+n), \tag{A4}$$

$$G^3_{m,n}(\mathbf{R}_n,\mathbf{R}_m) = G(\mathbf{R}_n,\mathbf{R}_m;m+n+2N_1), \tag{A5}$$

$$G^4_{m,n}(\mathbf{R}_n,\mathbf{R}_m) = G(\mathbf{R}_n,\mathbf{R}_m;m-n+N_1), \tag{A6}$$

$$G^5_{m,n}(\mathbf{R}_n,\mathbf{R}_m) = G(\mathbf{R}_n,\mathbf{R}_m;m+n+N_1), \tag{A7}$$

where

$$G(\mathbf{R}_n,\mathbf{R}_m;\alpha) = \left(\frac{3}{2\pi a^2|\alpha|}\right)^{(3/2)}\exp\left\{-\frac{3(\mathbf{R}_m-\mathbf{R}_n)^2}{2a^2|\alpha|}\right\}. \tag{A8}$$

Substituting these expressions in Eq. (A2) and taking the continuos limit by transforming the sums into integrals we find the structure factor for the dendrimer of two generations

$$\begin{aligned} S_2(\mathbf{q}) = {} & \frac{N_1}{N_1+2N_2}S_1(\mathbf{q}) + \frac{2N_2}{N_1+2N_2}\left[\frac{N_2}{x_2^2}(\exp\{-x_2\}-1)^2\right. \\ & \left. + \frac{2N_2}{x_2^2}(\exp\{-x_2\}-1+x_2)\right] + \frac{2N_2}{N_1+2N_2}\left[\frac{2N_2}{x_2^2}(P_0\right. \\ & \left. -1)\exp\{-2x_1\}(\exp\{-x_2\}-1)^2\right] \\ & + \frac{2N_2}{N_1+2N_2}\frac{2N_2}{x_2^2}[1+(P_0-1)\exp\{-x_1\}] \\ & \times(\exp\{-x_1\}-1)(\exp\{-x_2\}-1), \end{aligned} \tag{A9}$$

where

$$S_1(\mathbf{q}) = \frac{(P_1-1)N_1}{x_1^2}(\exp\{-x_1\}-1)^2 + \frac{2N_1}{x_1^2}(\exp\{-x_1\}-1+x_1), \tag{A10}$$

is the structure factor of a star of P_1 arms and N_1 monomers [18]. This expression contains two terms. The first term of the right-hand side expresses cross correlations between the different arms of the star. The second term refers to the normal Debye function for a linear polymer of N_1 monomers, as found by taking the appropriate limit $P_1=1$. Note that the general procedure explained above can be easily generalized to calculate the structure factors of general branched structures like those studied in this paper.

APPENDIX B: SUMMARY FOR THE SCALING REGIMES

In this appendix we summarize the results for the scaling regimes of the branched and hyperbranched structures studied in this work and write them using a simpler notation. (a), (b), (c), and (d) show the results for Gaussian polydisperse stars, self-avoiding walk (SAW) polydisperse stars, Gaussian dendrimers and SAW dendrimers, respectively.

First intermediate regime $S(q)\sim q^{-s}$:

(a) $s=4(1-1/2m)$
(b) $s=\frac{10}{3}(1-2/(6m-1))$
(c) $s=4(1+1/2m)$
(d) $s=\frac{10}{3}(1+2/(6m+1))$.

Transition points between the Guinier and the first intermediate regime:

(a) $(qR_g)^2\sim 1$
(b) $(qR_g)^{5/3}\sim 1$
(c) $(qR_g)^2\sim 1$
(d) $(qR_g)^{5/3}\sim 1$.

Transition points between the first and second intermediate regimes:

(a) $(qR_g)^2\sim N_{max}/N_{min}$
(b) $(qR_g)^{5/3}\sim N_{max}/N_{min}$
(c) $(qR_g)^2\sim \mathcal{N}_{max}/\mathcal{N}_{min}$
(d) $(qR_g)^{5/3}\sim \mathcal{N}_{max}P_G^{1/3}/\mathcal{N}_{min}P^{1/3}$.

Transition points between the second intermediate regime and the region where fluctuations dominate:

(a) $(qR_g)^2\sim P(N_{max}/N_{min})^{1/m}$
(b) $(qR_g)^{5/3}\sim P^{2/3}(N_{max}/N_{min})^{4/(6m-1)}$
(c) $(qR_g)^2\sim P_G(\mathcal{N}_{max}/\mathcal{N}_{min})^{-1/m}$
(d) $(qR_g)^{5/3}\sim P_G^{2/3}(\mathcal{N}_{max}P_G^{1/3}/\mathcal{N}_{min}P^{1/3})^{-4/(6m+1)}$.

Transition points between the first intermediate regime and the region where fluctuations dominate:

(a) $(qR_g)^2\sim P^{m/(m-1)}$
(b) $(qR_g)^{5/3}\sim P^{(2/3)(6m-1)/(6m-5)}$
(c) $(qR_g)^2\sim P_G^{m/(m+1)}$
(d) $(qR_g)^{5/3}\sim P_G^{(2/3)(6m+1)/(6m+5)}$.

[1] See, for example, M.R. Gittings, Luca Cipelletti, V. Trappe, D.A. Weitz, M. In, and C. Marques, J. Phys. Chem. B **104**, 4381 (2000).
[2] T.A. Witten and L.M. Sander, Phys. Rev. Lett. **47**, 1400 (1981).
[3] However see, C. Oh and C.M. Sorensen, Phys. Rev. E **57**, 784 (1998).
[4] P.G. de Gennes and H. Hervet, J. Phys. Lett. **44**, L351 (1983).
[5] M. Murat and G.S. Grest, Macromolecules **29**, 1278 (1996).
[6] E. Mendes, P. Lutz, J. Bastide, and F. Bou, Macromolecules **28**, 174 (1995).
[7] H.A. Al-Muallem and D.M. Knauss, J. Polym. Sci., Part A: Polym. Chem. **39**, 3547 (2001).
[8] D.M. Knauss, H.A. Al-Muallem, T. Huang, and D.T. Wu, Macromolecules **33**, 3557 (2000); D.M. Knauss and H.A. Al-Muallem, J. Polym. Sci., Part A: Polym. Chem. **38**, 4289 (2000); H.A. Al-Muallem and D.M. Knauss, *ibid.* **39**, 152 (2001).
[9] A. Sunder, J. Heinemann, and H. Frey, Chem.-Eur. J. **6**, 2499 (2000).
[10] Z. Muchtar, M. Schappacher, and A. Deffieux, Macromolecules **34**, 7595 (2001).
[11] C.M. Marques, D. Izzo, T. Charitat, and E. Mendes, Eur. Phys. J. B **3**, 353 (1998).
[12] M. Abramowitz and I.A. Stegun, *Handbook of Mathematical Functions* (Dover Publications Inc., New York, 1972), p. 297.
[13] M. Daoud and J.P. Cotton, J. Phys. (France) **43**, 531 (1982).
[14] Asymptotically, for very high arm number, the high q-regime of slope $-5/3$ does not cross over directly into the intermediate regime of slope $-10/3$ at $qR_{\mathrm{star}}=P^{2/5}$. In fact, the semidilute character of the corona shows up as a plateau for wave vectors smaller than the reciprocal of an average blob size $\xi \sim R_{\mathrm{star}}P^{-1/2}$. The scattering intensity should then be a constant in the range $P^{9/20} \ll qR_{\mathrm{star}} \ll P^{1/2}$. However, the ratio of the upper to the lower boundaries is only of the order of $P^{1/20}$, and therefore invisible under normal conditions.
[15] We study the limit of high number of arms and large number of arm sizes for which asymptotic shapes are well developed.
[16] Strictly speaking, Eq. (2) only leads to a scaling form if the integral there converges. This can be achieved by using a soft cutoff as for instance $\phi(r)=\exp(-r/r_{max})/r^{\mu}$. In this case $S(q) \sim q^{2(\mu-3)}(qr_{max})^{2(2-\mu)}(1+(qr_{max})^2)^{\mu-2}\Gamma^2(2-\mu)\sin^2 \times((2-\mu)\arctan(qr_{max}))$ for $\mu<3$. If $r_{max} \gg 1$ then $S(q) \sim q^{2(\mu-3)}$.
[17] T.J. Prosa, B.J. Bauer, and E.J. Amis, Macromolecules **34**, 4897 (2001).
[18] J.S. Higgins and H.C. Benoît, *Polymers and Neutron Scattering* (Oxford University Press, Oxford, 1996).